NUMERICAL INVESTIGATION OF FLEXIBLE BEAMS FOR ELECTROMAGNETIC ENERGY HARVESTING UNDER THE WAKES FROM UPSTREAM CYLINDER

Samir Chawdhury[*] **and Guido Morgenthal** [†]

[*] [†] Modelling and Simulation of Structures
Bauhaus University Weimar
Marienstr. 13, 99423 Weimar, Germany
e-mail: samir.chawdhury@uni-weimar.de, web page:
http://www.uni-weimar.de/Bauing/MSK/-en.html

Key words: Electromagnetic energy harvesting, Low wind speed harvesters, Wake flows, Upstream wakes, Vortex Particle Methods, Wireless sensor, Structural health monitoring.

Abstract. The paper investigates the potential of flexible cantilever beams numerically for electromagnetic (EM) energy harvesting under the wakes from upstream cylinder. A two-dimensional fully coupled fluid–structure interaction model has been presented. The flow solver based on the Vortex Particle Method and the structural solver based on corotational finite element formulation are coupled to accurately account for the geometrically nonlinear effects of such very flexible elements. A reference flutter-based harvester is simulated initially for the validation of the solver. The coupled solver is used furthermore to model the power output from the flexible cantilever beam under the wakes from the upstream circular cylinder, particularly, at low wind speeds like 2-4 m/s. Satisfactory results are achieved while the modeled energy outputs of the proposed harvester model are compared with the reference harvester.

1 INTRODUCTION

In recent years, energy harvesting from ambient vibration sources for wireless sensor nodes (WSN) has been extensively investigated, particularly, to replace the conventional use of expensive batteries. With the rapid advancements in wireless technologies and low-power electronics, the power consumption of electronic devices has been reduced to a few milliwatts. Wind energy offers an alternative source of mechanical vibration which can be converted into electrical energy. Structures under wind loading may experience large vibration due to the aerodynamic phenomena like vortex-induced vibration (VIV), galloping, flutter, etc. Akaydin exploited the vibration of the flexible beam under different wind fields in [1] for piezoelectric energy harvesting. The transverse galloping of bluff

523

sections was utilized in [2] and [3] for piezoelectric induction. On the other hand, the VIV phenomenon was used in [4] for electromagnetic (EM) power generation. The wind-induced vibration of stay cables has been investigated in [5] for EM power generation. The instability phenomena galloping was used by [6] and [7] for EM induction. The susceptibility of the T-shaped cantilever system to rotational flutter was used for EM power generation in [8].

This paper presents a two–dimensional fully coupled fluid–structure interaction (FSI) model for simulating flexible cantilever beams to investigate numerically the potential of electromagnetic (EM) energy harvesting under the wakes from upstream cylinder. The numerical investigations within this study have been carried out using a Computational Fluid Dynamic (CFD) solver VXflow, which is fundamentally based on Vortex Particle Method (VPM). The solver has successfully been used for modeling of flows past complex structural assemblies in [9], [10] as well as for simulation of bridge aerodynamics in [11]. A structural solver based on a corotational finite element formulation is coupled with the mentioned CFD solver to model the large deformation effects.

The energy in the wakes, generated from upstream cylinder under free stream flow, can be used for small-scale energy harvesting [12]. If the resonance frequency of a flexible cantilever system in the downstream become same as the frequency of the upstream vortex shedding, the structure may experience large amplitude vibrations. The potential of conversion of this mechanical vibration into electrical energy using an EM transducer has been studied here numerically. In this study, a T-shaped harvester based on instability phenomenon flutter, which was investigated extensively for EM power generation in [8], has been considered as the reference system and also used for the validation of the proposed coupled solver. Numerical simulations are performed using the validated coupled solver to investigate the efficiency of the proposed harvester model, particularly, under low wind speed in contrast to the reference flutter-based harvester.

2 ELECTROMAGNETIC ENERGY HARVESTING FROM WAKES

2.1 Design of the energy harvester

The vibration of flexible cantilever system under the wakes from upstream circular cylinder has been proposed for electromagnetic (EM) energy harvesting. When the vortex shedding frequency (f_s) of an upstream cylinder comes close to the resonance frequency of the downstream cantilever beam (f_α), large vibration may occur. Using an EM transducer, it is possible to create the required relative movement between magnet and coil for EM power generation. The energy harvesting mechanism from upstream wakes using a prototype flexible cantilever system is presented schematically in Figure 1. For a circular cylinder, the frequency of the vortex shedding can be expressed as [13]:

$$f_s = \frac{StU_\infty}{D} \tag{1}$$

where St is the Strouhal number, U_∞ is the free stream flow, and D is the diameter of the
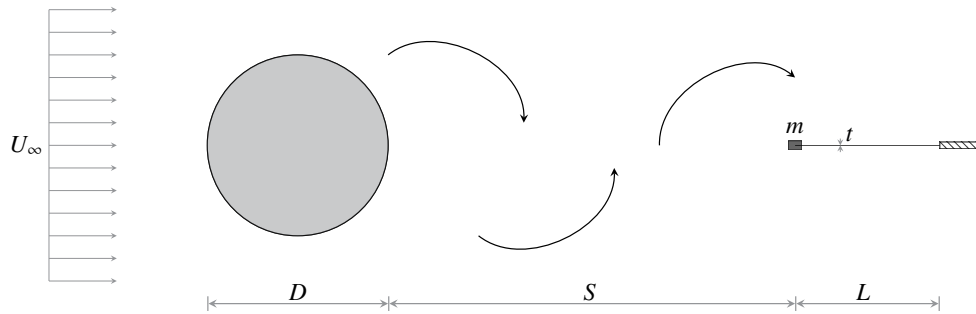
Figure 1: Schematic electromagnetic energy harvesting from wakes from upstream cylinder: an upstream circular cylinder of diameter D generates wakes under the free stream flow U_∞. A downstream flexible cantilever beam, with a magnet of mass m at the cantilever tip, is located at a distance S from the upstream cylinder. Here, t and L are the thickness and the length of the cantilever harvester.
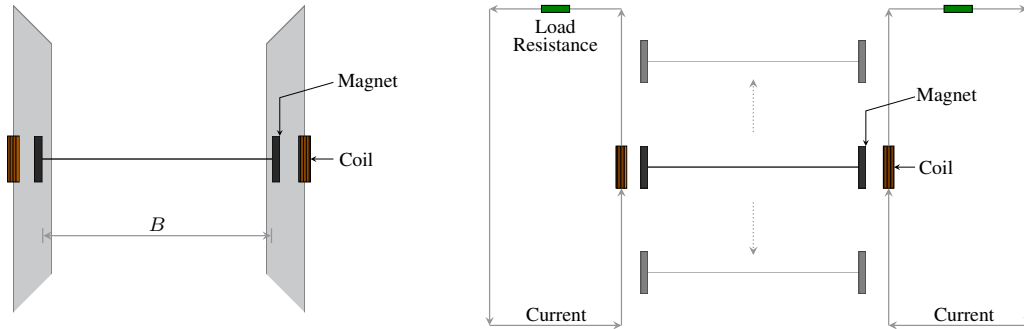

Figure 2: Conversion of mechanical vibration of the flexible cantilever beam in c.f. Figure 1 into electrical power using an electromagnetic transducer: (left) front view and the coils attached to the side walls, (right) the current flow in the circuit due to the relative movement between the magnets and coils.

circular cylinder. For a wide range of high Reynolds number (Re), the strouhal number of circular cylinder is almost constant, which is 0.2 [14]. The Re of a circular cylinder for a free stream flow can be expressed as following:

$$Re = \frac{U_\infty D}{\nu} \tag{2}$$

where ν is the kinematic viscosity of the fluid. Under specific free stream flow, the frequency of vortex shedding depends on the dimension of the circular cylinder. Therefore, to target a specific wind speed for energy harvesting, the options are to change cylinder size and/or to change the system frequency such that f_s and f_α become close to each other. Figure 2 shows the electromagnetic configuration of the proposed harvester. At the resonance state, the vibration of the tip of the cantilever beam causes a relative movement between the magnet and the coil and induces current flow through the circuit. The side walls are provided not only to hold the coils but also to keep the wakes flows less affected along the width of the harvester.

2.2 Concepts of electromagnetism

The fundamental principle of electromagnetism is that the relative movement between magnet and coil results in a varying amount of magnetic flux cutting through the coil. According to Faraday's law of induction, the open-circuit voltage V_{oc} in the loop of the coil can be expressed as follows [15]:

$$V_{oc} = \oint_{l_{coil}} (v \times \beta)\, dl = NlBv, \tag{3}$$

where, B is the magnetic flux density at each coil segment, dl is the vector of each segment of the coil, l_{coil} is the total length of the coil, v is the relative velocity between the center of the coil and the magnet, N is the number of coil turns, and l is the mean circumference of the coil. The Voltage across the load resistance, V_L, can be calculated as follows

$$V_L = V_{oc} \frac{R_L}{R_L + R_C} \tag{4}$$

where R_L and R_C are the load resistance and coil resistance, respectively.

3 FULLY COUPLED CFD SOLVER

3.1 Vortex Particle Method

The Vortex Particle Method (VPM) is fundamentally based on the simplified vorticity description of the fundamental Navier-Stokes (NS) equation. For incompressible unsteady flow of a viscous fluid, the NS equation in terms of the vorticity can be expressed as:

$$\frac{\partial \omega}{\partial t} + (\boldsymbol{u} \cdot \nabla)\, \omega = \nu \nabla^{\mathbf{2}} \omega. \tag{5}$$

For inviscid flow equation (5) can be rewritten in substantial derivative notation such that

$$\frac{\mathrm{D}\omega}{\mathrm{D}t} = 0. \tag{6}$$

Here, equation (6) allows the use of gridless numerical scheme and discretization of particle elements in Lagrangian manner. Further details on the method can be found in [9, 11].

3.2 Structural model

The structural system is modeled as multi-degree of freedom (MDOF) system, in which the system is subdivided into a number 2-D Euler–Bernoulli finite beam elements. The equation of motion for a system with many degrees of freedom can be written as

$$\mathbf{M}\ddot{X} + \mathbf{C}\dot{X} + \mathbf{K}X = F. \tag{7}$$

where $X, \dot{X}, \ddot{X}$ are the vector of nodal displacements, velocities and accelerations respectively; and $\mathbf{M}$, $\mathbf{C}$, $\mathbf{K}$ are the mass, structural damping and stiffness matrix respectively;

and F is the force vector. The damping of the system is approximated based on the assumption of Rayleigh damping approach as follows

$$\mathbf{C} = a_0\mathbf{M} + a_1\mathbf{K} \tag{8}$$

where, a_0 and a_1 are proportionality factor for mass-proportional and stiffness-proportional damping, respectively. As solution algorithm, the commonly used Newton–Raphson algorithm is used. The Newmark-Beta method is employed as the numerical integrator.

3.3 Fluid-structure coupling

At each simulation time step, the calculated pressures on the surface panels from the flow solver are projected into nodal forces for the structural solver. After achieving the solution of the deformed structure, the surface panels and the panel velocities are calculated by projecting the nodal solutions, and supplied to the flow solver. The recalculation of the surface vortices for the updated surface panels are then performed by the flow solver. Finally, the boundary conditions are updated to perform further calculations in loops.

4 MODELING OF ELECTROMAGNETIC ENERGY HARVESTERS

4.1 Introduction

This section presents the utilization of the presented coupled solver for simulating the flexible cantilever beam under the wakes from upstream circular cylinder. The aim is to model the extracted energy outputs from the vibration of the proposed cantilever harvester using an electromagnetic (EM) transducer. However, to understand the efficiency of the proposed harvester model, a flutter-based T-shaped cantilever harvester, which was studied in [8], has been considered as reference harvester. The presented coupled solver is validated initially by comparing the modeled energy outputs with the reference harvester. Furthermore, the validated solver has been shown used to model the proposed EM energy harvesting from upstream wakes. The optimization of the performance of the proposed harvester is also investigated.

4.2 Modeling of T-shaped reference harvester for solver validation

The equation of motion of the prototype harvester considering the influence of electromagnetic transducer can be expressed as follows

$$\mathbf{M}\ddot{X} + (\mathbf{C}_m + \mathbf{C}_e)\dot{X} + \mathbf{K}X = F, \tag{9}$$

where $\mathbf{C}_m + \mathbf{C}_e$ represents the system damping matrix within the framework of the structural solver, c.f. equation (8). The proportional factors, a_0 and a_1, are calculated considering the first two vibration modes of the harvester (ω_1 and ω_2) using equation (10),

$$a_0 = \zeta_t \frac{2\omega_1\omega_2}{\omega_1 + \omega_2}, \ a_1 = \zeta_t \frac{2}{\omega_1 + \omega_2}, \tag{10}$$

where ζ_t is the total system damping ratio. The physical dimensions and the dynamic proerties of the reference T-shaped harvester and also the proposed harvester in Figure 1 are shown together in Table 1. The only difference is that the reference harvester has a vertical plate of height H at the cantilever tip. The damping ratios ($\zeta_t = \zeta_m + \zeta_e(R_L)$) of the reference harvester for different electrical load resistances R_L (100–5000 Ω) were measured experimentally by performing free vibration tests. The corresponding total system damping coefficients ($c_t = c_m + c_e(R_L)$) were calculated using the following equation

$$c_t = c_m + c_e(R_L) = 2m_\alpha(\zeta_m + \zeta_e(R_L))\omega_\alpha, \tag{11}$$

where m_α and ω_α are the rotational mass and frequency of the system. Here, for a cantilever beam with tip mass m, the natural frequency and the rotational stiffness of the system can be calculated using $\omega_\alpha = \sqrt{3EI/mL^3}$ and $K_\alpha = 2EI/L^2$, respectively. The effective rotational mass can be calculated using $m_\alpha = K_\alpha/\omega_\alpha^2$. It is also possible to express the total system damping as follows:

$$c_t = c_m + c_e(R_L) = 2m_\alpha\omega_\alpha\zeta_m + \frac{(NlB)^2}{R_L + R_C}, \tag{12}$$

where the term $R_L + R_C$ in equation (12) indicates the sum of the electrical load resistances and the coil resistances from two sets of closed circuits with magnets and coils. NlB is the electromagnetic transformation factor.

Here, the proposed coupled solver has been used to model the reference T-shaped cantilever harvester. The discretization of the harvester within the framework of the flow and the structural solver has been shown schematically in Figure 3. The non-dimensional size of the boundary element Δ_s for flow solver is chosen such that $\Delta_s/H = 0.05$. The structural solver employs a 2-D finite element formulation to model the prototype harvester. The system is discretized into 62 idealized finite beam elements such that the length of each element is $0.05H$. The two-node elastic beam–column element is used where each node has three degrees of freedoms, which are the translation in horizontal and vertical directions, and in-plane rotation. The mass of the cantilever system is distributed into 63 structural nodes; consequently, the lumped mass at each structural node is assigned 2.39×10^{-5} kg approximately. The mass of the magnet M is assigned at the cantilever tip. The selection of the global time step of the coupled simulation is governed by the time step of the flow solver Δt_f, which is equal to Δ_s/U_∞. On the contrary, the initial time step of the structural solver Δt_s is considered equal to that of the flow solver Δt_f.

Table 1: Physical dimensions and dynamic properties of the prototype harvester.

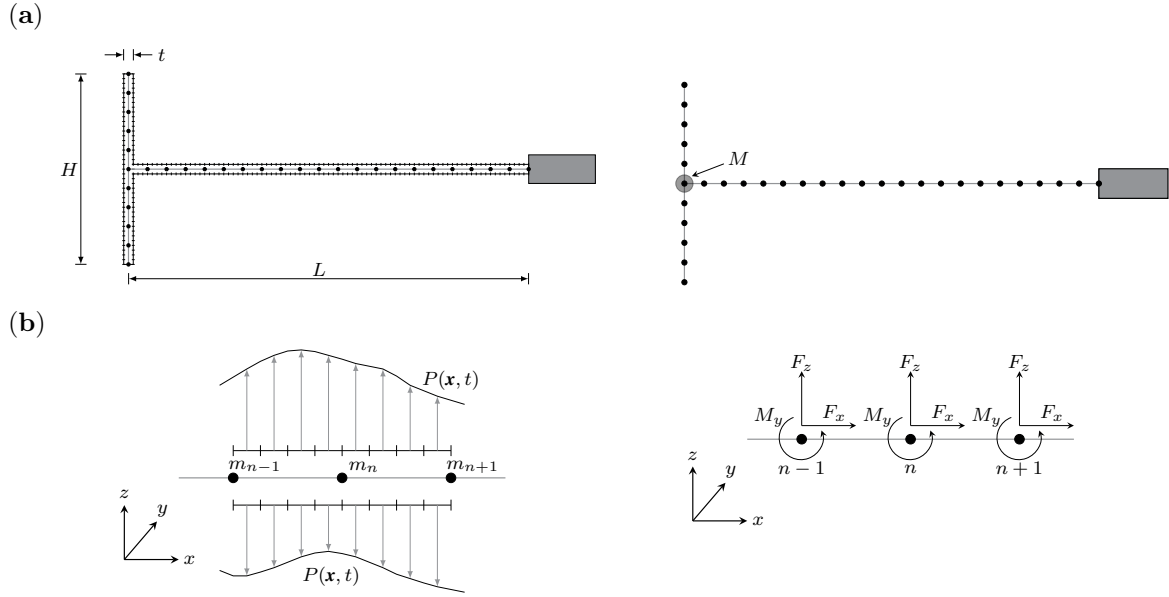|	
$B = 0.03$ m, $L = 0.042$ m	H (tip height of T-shape harvester) = 0.02 m
t (thickness) $= 1.016 \times 10^{-4}$ m	M (mass of the magnet) = 0.009 kg
E (modulus of elasticity) = 180 GPa	I (moment of inertia) $= 2.62 \times 10^{-15}$ m^4
ω_α (natural frequency) = 46.1 rad/sec	ζ_m (mechanical damping ratio) = 0.004

(**a**)

(**b**)

Figure 3: Discretization scheme of the coupled CFD solver in terms of the T-shaped cantilever harvester: (a-left) the discretization of the harvester in flow solver and the structural solver together, (a-right), structural nodes, idealized finite beam elements, lumped masses, and magnet M, (b-left) pressure distribution on surface panels, and (b-right) projected nodal forces for the structural solver.
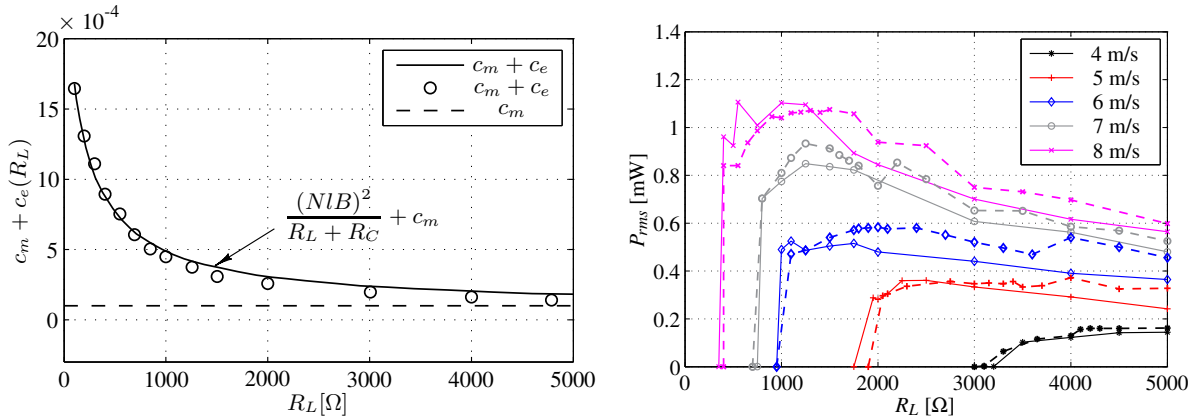

Figure 4: Damping of the reference prototype T-shaped harvester for different electrical load resistances [8]: (left) (∘) shows the experimentally measured total damping, while (——) indicates the fitted total system damping. (− − −) represents the mechanical damping only. (right) Comparison of RMS power outputs from CFD simulations (——) with the reference wind tunnel test results (- - -).

A further subdivision into smaller time steps is performed to achieve the convergence of the structural solution. The simulations are performed at different wind speeds (4–8 m/s) under different R_L (100–5000 Ω). The total damping factors measured experimentally in [8] for different R_L are presented in Figure 4 (left). The resistance of the coil R_C was

measured 130 Ω. The average transformation factor NlB is calculated here approximately equal to 1.02 from the fitted damping factors in Figure 4 (left). The voltage across the load resistance, V_L is measured from individual simulation and corresponding root mean square (RMS) power output (P_{rms}) is computed from V_{Lrms} (i.e. V_{Lrms}^2/R_L). Finally, for different wind speeds and R_L, the modeled power outputs are compared in Figure 4 (right) and the results are found satisfactory. More detailed investigations on the reference harvester and and discussions have been presented in [16].

4.3 Modeling of proposed harvester under wakes from upstream cylinders

The validated coupled solver has been employed here to simulate the proposed cantilever harvester under the wakes coming from upstream circular cylinder, c.f. Figure 1. For numerical simulations, the physical dimensions and the mechanical properties of the harvester are considered according to the reference harvester, c.f. Table. 1. In this study, the vertical tip plate of the reference harvester has been removed. Note, it is observed in [8] that at or below the wind speed of 7 m/s for $R_L = 750$ Ω, the T-shaped harvester produced no energy output, c.f. Figure 4 (right). The system damping, which is sum of the mechanical and electrical damping, increases with the reduction in load resistance, c.f. Figure 4 (left). Therefore, for a flutter-based harvester the increment in the system damping necessitates high wind speed for extracting power output. In contrast, the proposed harvester should be able to extract energy at low wind speeds since it exploits the resonance phenomena. Therefore, the interest is to investigate the potential of the proposed harvester considering $R_L = 750$ Ω under wind speed less than 4 m/s. So, the diameter of the upstream circular cylinder D is chosen 0.1 m, which is kept more than twice the length of the harvester, particularly, to reduce the influence of the harvester vibration on upstream wake generation. To induce resonance, it is considered that the vortex shedding frequency f_s is equal to the frequency of the harvester ($f_\alpha = \omega_\alpha/2\pi = 7.34\ Hz$). Then, for chosen circular cylinder with $St = 0.2$ the critical free stream flow U_∞ is calculated 3.67 m/s using equation (1). The corresponding Re according to equation (2) is calculated approximately 25,000 which justifies the consideration of St value of 0.2.

The discretization of the harvester in flow and structural solver has been shown schematically in Figure 3, however, in this case without considering the vertical tip plate. The surface of the harvester and the upstream circular cylinder in the flow solver are discretized into a number of surface panels to solve the N–S equations. The non-dimensional size of these boundary elements for harvester and the cylinder are chosen such that $\Delta_s/D = 0.0097565$. The cantilever beam is discretized into 43 nodal points such that each idealized FE beam length become $0.01D$. The lumped mass approach has been used to approximate the nodal mass of the system. The mass of the cantilever beam is lumped into 43 nodes, in which nodal mass for each node is approximately 2.39e-5 kg. The flexible cantilever harvester is simulated under the wakes coming from upstream circular cylinder at free stream velocity U_∞ of 3.67 m/s. In this study, for $R_L = 750$ Ω the system damping matrix ($\mathbf{C}_m + \mathbf{C}_e$) is calculated using the Rayleigh damping approach according to
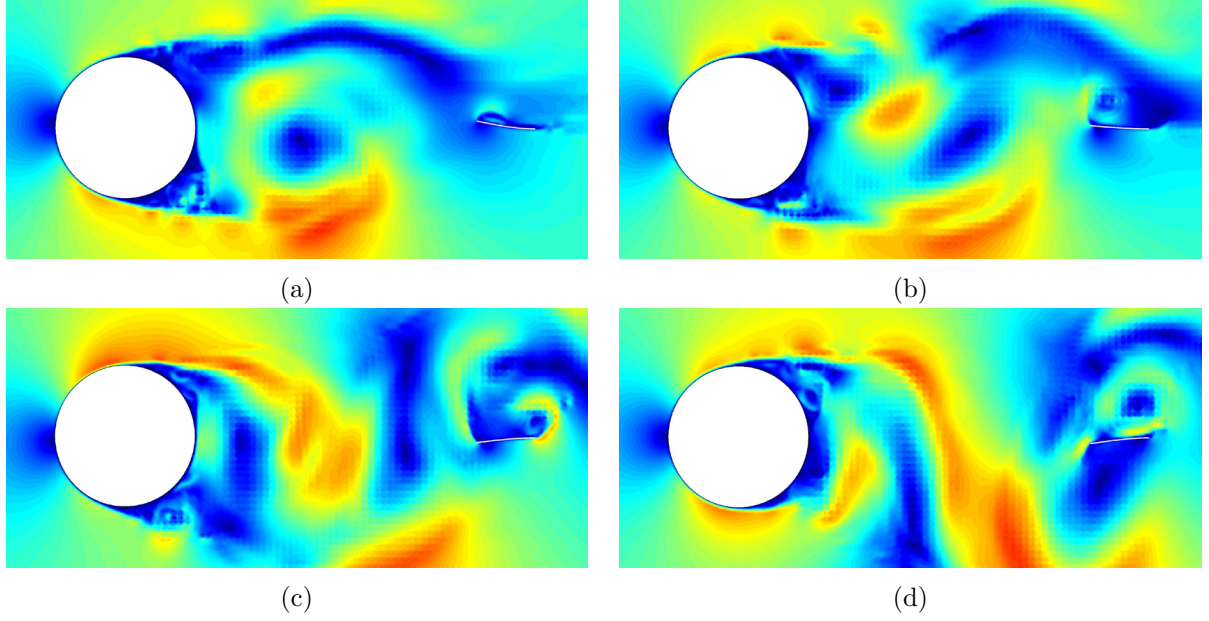
Figure 5: Simulation of proposed harvester under wakes from upstream cylinder at free stream flow of 3.67 m/s. The snapshots of the flow field are shown for case $S = 2D$ and the vibration of the beam at different real times such that (a) $t = 2.6505$ s, (b) $t = 2.6769$ s, (c) $t = 2.7035$ s, and (d) $t = 2.7299$ s.

equation (8). The damping ratio for chosen R_L has been calculated using equation (11) to calculate the Rayleigh damping factors. In four different simulations, the distance between the cylinder and the harvester has been considered $1D, 1.5D, 2D$, and $2.5D$ to investigate their influences on the system vibration. The simulated flow fields and system vibration for case $S = 2D$ are shown in Figure 5 for different simulation steps. For all the simulation cases, the vertical cantilever tip displacements and the corresponding modeled voltages, which is using equation (4), are presented in Figure 6. It is observed that the proposed harvester is producing voltage output for all the cases, and comparatively better for the cases $2D$, and $2.5D$, whereas the reference harvester under the same condition produced no output. The maximum power output P_{max}, which is $V_{L_{max}}^2/R_L$, is observed for case $S = 2D$ approximately 0.15 mW, whereas the root mean square power P_{rms} is observed approximately 0.085 mW for the simulated time.

4.4 Optimization of the performance for proposed harvester

In this section, the performance of the proposed harvester is analyzed by targeting low wind speed like 2–4 m/s since the flutter-based harvesters are generally more efficient at high wind speeds [8]. The wind speed for the proposed harvester can be targeted by modifying the physical configuration of the harvester and/or by modifying the diameter of the upstream cylinder such that the frequency of the vortex shedding and the natural frequency of the harvester corresponds with each other. The two key parameters to target
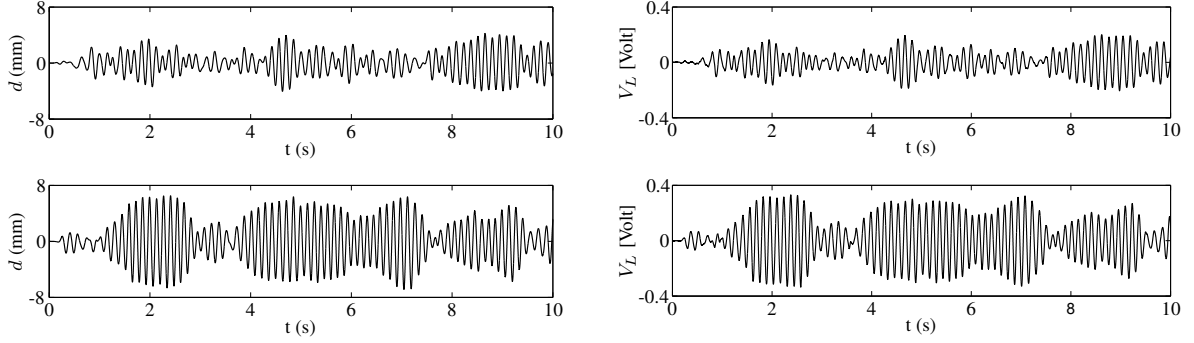
Figure 6: Comparison of vertical tip displacement and voltage output of the harvester under wakes from upstream cylinder ($U_\infty = 3.67$ m/s, $D = 0.10$ m): (top) $S = 1D$ and (bottom) $S = 2D$

a specific wind speed is the diameter of the upstream cylinder and the frequency of the downstream cantilever system.

For a target free stream flow U_∞ using a circular cylinder of diameter D, the frequency of the harvester should be equal to the frequency of vortex shedding such that $f_\alpha = f_s = (U_\infty St)/D$. The length of the harvester L is increased to 0.08 m to allow the cantilever tip to vibrate more for increasing the velocity of vibration (length of the reference harvester was 0.042 m). Accordingly, the diameter D of the upstream cylinder is increased to 0.15 m to reduce the influence of the beam vibration on the wakes generation. The numerical simulations are performed here for wind speed U_∞ of 2, 3, and 4 m. The diameter of the circular cylinder is considered constant for these studied wind speeds. The thickness of the harvester is modified such that the harvester frequency matches with the frequency of vortex shedding under individual wind speed. The vortex shedding frequencies for wind speeds 2, 3, and 4 m/s are calculated 2.66 Hz, 4 Hz, and 6 Hz, respectively. The corresponding thickness of the harvesters are modified to 0.1005 mm, 0.13165 mm, and 0.1725 mm, respectively. Here, the energy harvesters are referred as EH-1, EH-2, and EH-3, respectively. The tip mass of the cantilevers, i.e. the magnet mass, is considered 0.009 Kg according to the reference harvester, c.f. Table 1. The mass of the cantilever beam is lumped into 81 nodes, in which nodal mass for each node is approximately 2.43e-5 kg, 3.1e-5 kg and 4.06e-5 kg respectively for EH-1, EH-2, and EH-3. To maximize the power output, the harvesters are simulated for system damping considering R_L of 100 Ω. Since the studies are performed for low R_L, the resistances of the coil R_C is necessarily should be very low, and hence, is neglected to maximize the voltage. The total system damping ratio $(\zeta_m + \zeta_e(R_L))$ of the harvesters are calculated based on equation (11) using Figure 4 (left) and they are calculated 0.119, 0.081, and 0.055, respectively. The estimated root mean square (RMS) voltage and power outputs are compared for different wind speeds in Figure 7. It is observed that the power output of the harvester EH-3 under wind speed 4 m/s is found approximately 0.84 mW which is almost the harvested power output of the reference harvester at wind speed 7 m/s [8].
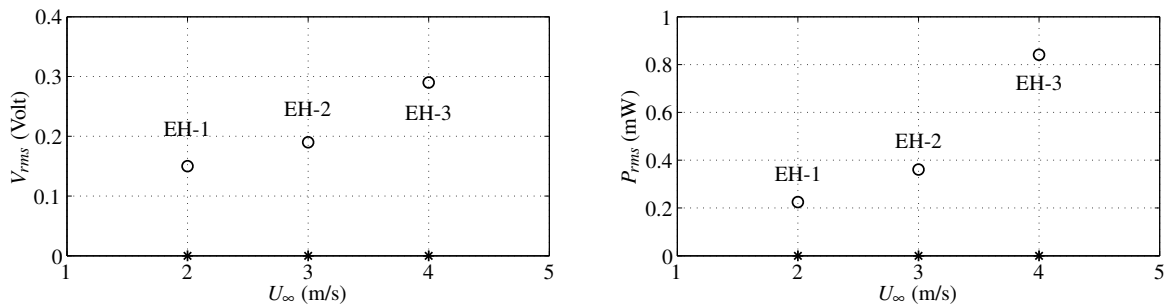
Figure 7: Comparison of modeled energy outputs of modified harvesters with reference harvester at R_L = 100 Ω: (a) RMS voltage (b) RMS power. Here, (∗) indicates the power output of reference harvester.

5   CONCLUSION

The performance of a flexible cantilever beam for electromagnetic (EM) energy harvesting under the wakes from upstream cylinder has been investigated using a proposed two–dimensional fully coupled fluid–structure interaction model. The modeling scheme and validation of the proposed coupled solver have been presented. A flexible cantilever beam can experience large vibration, especially, when the frequency of the vortex shedding from upstream cylinder comes close to the resonance frequency of the system. This fact is exploited in this paper to investigate numerically the potential of a flexible beam for EM energy harvesting under the wakes from upstream circular cylinder. The influential parameters such as the upstream cylinder diameter, the frequency of the downstream harvester and the distance between them have been studied and the results are discussed. The position of the downstream cantilever beam at a distance of twice the diameter of the cylinder diameter has been found more effective for power extraction. It is shown in this study that by changing the harvester frequency or by modifying the cylinder size, it is possible to target a specific wind speed for energy harvesting. However, the focus of the paper is concentrated particularly for harvesting energy from low wind speed like 2–4 m/s. The harvested energy outputs are found satisfactory in comparison with a reference flutter-based EM energy harvester. The ability of the proposed harvester model to extract energy from low wind speed would make it possible to harvest energy for a wide range wind speeds while using the flutter-based harvesters to target the high wind speed.

REFERENCES

[1] Akaydin, H.D., Elvin, N. and Andreopoulos, Y. (2012) The performance of a self-excited fluidic energy harvester. *Smart Materials and Structures* 21(2): 025007.

[2] Abdelkefi, A., Hajj, M.R., and Nayfeh, A.H. (2012) Power harvesting from transverse galloping of square cylinder. *Nonlinear Dynamics*, 70(2), pp.1355-1363.

[3] Ewere, F. and Wang, G. (2013) Performance of galloping piezoelectric energy harvesters. *Journal of Intelligent Material Systems and Structures*, 25(14), pp.1693-1704.

[4] Wang, D.A., Chiu, C.Y., and Pham, H.T. (2012) Electromagnetic energy harvesting from vibrations induced by Kármán vortex street. *Mechatronics* 22.6: 746-756.

[5] Jung, H.J., Kim, I.H. and Jang, S.J. (2011) An energy harvesting system using the wind-induced vibration of a stay cable for powering a wireless sensor node. *Smart Materials and Structures*, 20(7), p.075001.

[6] Dai, H.L., Abdelkefi, A., Javed, U. and Wang, L. (2015) Modeling and performance of electromagnetic energy harvesting from galloping oscillations. *Smart Materials and Structures*, 24(4), p.045012.

[7] Vicente-Ludlam, D., Barrero-Gil, A., and Velazquez, A. (2014) Optimal electromagnetic energy extraction from transverse galloping. *Journal of Fluids and Structures*, 51, pp.281-291.

[8] Park, J., Morgenthal, G., Kim, K., Kwon, S.D. and Law, K.H. (2014) Power evaluation of flutter-based electromagnetic energy harvesters using computational fluid dynamics simulations, *Journal of Intelligent Material Systems and Structures*, 25(14), 1800-1812.

[9] Morgenthal, G. and Walther, J.H. (2007) An immersed interface method for the vortex-in-cell algorithm. *Computers and structures* 85.11: 712-726.

[10] Chawdhury, S. and Morgenthal, G. (2016) Flow reproduction using Vortex Particle Methods for simulating wake buffeting response of bluff structures. *Journal of Wind Engineering and Industrial Aerodynamics*, 151, pp.122-136.

[11] Morgenthal, G. (2002) Aerodynamic analysis of structures using high-resolution vortex particle methods *PhD Thesis, University of Cambridge, Cambridge.*

[12] Akaydin, H.D., Elvin, N., and Andreopoulos, Y. (2010) Energy harvesting from highly unsteady fluid flows using piezoelectric materials. *Journal of Intelligent Material Systems and Structures*, 21(13), pp.1263-1278.

[13] Xu, Y.L. (2013) Wind effects on cable-supported bridges. *John Wiley and Sons.*

[14] Panton, R.L. (2006) Incompressible flow. 2nd edn, *John Wiley & Sons*, Inc., New York.

[15] Priya, S. and Inman, D.J. eds. (2009) Energy harvesting technologies (Vol. 21). New York: Springer.

[16] Chawdhury, S. and Morgenthal, G. (2017) Numerical simulations of aeroelastic instabilities to optimize the performance of flutter-based electromagnetic energy harvesters, *Journal of Intelligent Material Systems and Structures*, under review.